Ultrasonics 94 (2019) 382–390

Contents lists available at ScienceDirect

Ultrasonics

journal homepage: www.elsevier.com/locate/ultras

Improving broadband ultrasound attenuation assessment in cancellous bone by mitigating the influence of cortical bone: Phantom and in-vitro study

Yuriy Tasinkevych[a,*], Katarzyna Falińska[a], Peter A. Lewin[b], Jerzy Litniewski[a]

[a] Department of Ultrasound, Institute of Fundamental Technological Research of the Polish Academy of Sciences, Warsaw, Poland
[b] Drexel University, Philadelphia, PA 19104, USA

ARTICLE INFO

Keywords:
Broadband ultrasound attenuation
Correction of influence of cortical bone
Trabecular bone

ABSTRACT

The purpose of this work was to present a new approach that allows the influence of cortical bone on non-invasive measurement of broadband ultrasound attenuation (BUA) to be corrected. The method, implemented here at 1 MHz makes use of backscattered signal and once refined and clinically confirmed, it would offer an alternative to ionizing radiation based methods, such as DEXA (Dual-energy X-ray absorptiometry), quantitative computed tomography (QCT), radiographic absorptiometry (RA) or single X-ray absorptiometry (SXA), which are clinically approved for assessment of progress of osteoporosis. In addition, as the method employs reflected waves, it might substantially enhance the applicability of BUA - from being suitable to peripheral bones only it would extend this applicability to include such embedded bones as hip and femoral neck. The proposed approach allows the cortical layer parameters used for correction and the corrected value and parameter of the cancellous bone (BUA) to be determined simultaneously from the single (pulse-echo) bone backscattered wave; to the best of the authors' knowledge such approach was not previously reported. The validity of the method was tested using acoustic data obtained from a custom-designed bone-mimicking phantom and a calf femur. The relative error of the attenuation coefficient assessment was determined to be 3.9% and 4.7% for the bone phantom and calf bone specimens, respectively. When the cortical shell influence was not taken into account the corresponding errors were considerably higher 8.3% (artificial bone) and 9.2% (calf femur). As indicated above, once clinically proven, the use of this BUA measurement technique in reflection mode would augment diagnostic power of the attending physician by permitting to include bones, which are not accessible for transmission mode evaluation, e.g. hip, spine, humerus and femoral neck.

1. Introduction

The purpose of this work was to present a new single (pulse-echo based) measurement method that allows the influence of cortical bone (forming the outer layer of the cancellous interior) on broadband ultrasound attenuation (BUA) of cancellous bone (performed here at the frequency of 1 MHz) to be corrected. Once clinically confirmed, this approach would offer an alternative to ionizing radiation based methods, such as DEXA (Dual-energy X-ray absorptiometry) [1], quantitative computed tomography (QCT)[2], radiographic absorptiometry (RA) [3] or single X-ray absorptiometry (SXA) [4], which are clinically approved for assessment of progress of osteoporosis. In addition, as the method employs reflected waves, it might substantially enhance the applicability of BUA - from being suitable to peripheral bones only it would extend this applicability to include such embedded bones as hip, spine, humerus and femoral neck.

The outcome of in-vitro experiments indicates that BUA is strongly correlated to bone microstructure (correlation coefficient $R = -0.79$, $p < 0.0001$ between BUA and trabecular spacing (Tb. Sp.)) [5], bone volume density ($R = 0.85$, $p < 0.0001$), and bone mineral density (BMD) ($R = 0.8$, $p < 0.0001$) [6].

It is also evidenced that potential vulnerability for osteoporosis related fractures of hip [7], wrist, vertebra, pelvis, and humerus [8] can be predicted. Thus, based on ultrasound transmission measurements through the heel done for 5662 elderly women (mean age 80.4 years), Hans et al. observed that a decrease of one standard deviation (SD) in BUA increased the risk of hip fracture two-fold [7]. Also, based on heel scanning of 3180 women between the ages of 45 and 75 Thompson et al. concluded that a decrease of one SD in BUA increased the risk of wrist fracture by the factor of 1.6 [8].

Hip fractures are a major public health concern due to high morbidity, mortality, and healthcare expenses. A recent study [9] indicates that the incidence of hip fractures in older U.S. women is rising - from 2014 through 2015 the fracture rate in women ages 65–69 rose 2.5

* Corresponding author.
E-mail address: yurijtas@ippt.pan.pl (Y. Tasinkevych).

https://doi.org/10.1016/j.ultras.2018.06.018
Received 10 June 2018; Received in revised form 28 June 2018; Accepted 30 June 2018
Available online 02 July 2018
0041-624X/

percent, whereas rate for women between 70 and 74, rose 3.8 percent. The cost of the 11,000 additional estimated fractures from 2013 to 2015 alone was nearly $460 million, assuming a cost of $40,000 per hip fracture. The results presented in [9] corroborate the need for the development of an alternative – ideally, non-ionizing radiation based – approach to the x-ray DEXA method that is clinically approved. The work presented here recognizes that clinically acceptable osteoporotic fracture risk prediction by means of ultrasound depends on the correct determination of the BUA and the speed of sound (SoS), which are currently acquired in transmission mode. However, the transmission technique approach is limited to the peripheral bones, only-in practice, to the calcaneus and radius ones. Also, as osteoporotic changes may occur locally the diagnosis based on peripheral bones cannot be considered as representative for the whole skeleton [10]. Hence, as already alluded to, the existence of the alternative method applicable to bones, which are not accessible for through transmission mode i.e. for bones, which can be accessed from one side only (e.g. hip, spine, humerus etc.) would be of clinical importance.

A few attempts to obtain clinically useful information about bone quality using backscattered (pulse-echo (PE) mode) ultrasound were reported previously. These PE measurements permitted broadband ultrasound backscatter (BUB) [11], apparent integrated backscatter (AIB) [12], frequency slope of apparent backscatter (FSAB) and time slope of apparent backscatter (TSAB) [13] to be ascertained. The data were collected in several frequency bins. The frequency range of 0.2–0.6 MHz was used in calcaneus (BUB assessment) [11]. The bandwidth of 1–9 MHz implemented making use of 2 transducers operating at 3.5 and 5 MHz center frequencies yielded data for calcaneus (AIB assessment) [12], whereas FSAB and TSAB assessments in femoral head were determined in the frequency range between 0.5 and 15 MHz implemented with 5 different transducers having center frequencies of 1, 2.25, 5, 7.5, and 10 MHz [13].

In contrast to these methods the approach proposed here makes use of the pulse-echo (PE) mode to determine broadband ultrasound attenuation (BUA), which was not previously analyzed. In addition, the method presented offers enhanced sensitivity as it accounts for the shielding contribution of cortical bone. As evidenced below, such enhanced sensitivity might potentially pave way to be clinically applicable to assess the quality of such critical bones as hip, spine and humerus. As the cancellous bone is covered by a layer of cortical bone, the cortical shell distorts the measured BUA value by influencing the BUA frequency spectrum. The magnitude of this distortion depends upon the thickness of the cortex. This dependence was modeled and subsequently verified by Xia et al. in [14]. They noted that the cortical layer (of 1 mm thickness) accounted for approximately 15% of the BUA measured in-vitro in the frequency range from 0.3 MHz to 0.7 MHz. They also noted that this induced artifact was sensitive to the cortical shell thickness and increased (almost) linearly with increasing thickness [14]. Subsequently, the attempts were made to reduce the influence of bone cortex on the evaluation of cancellous bone BUA by measuring the trabecular structure cross-section coefficient or TSC. This coefficient was calculated as a ratio of the spectrum of the scattered signal to the spectrum of the transmitted signal [15], however, this approach is applicable in transmission mode, only.

The approach developed in this study allows the PE measurement of BUA to be conducted and the influence of the cortical bone on BUA assessment to be corrected from a single pulse-echo measurement, which allows the cortical bone parameters, such as its thickness, speed of sound (SoS), and cancellous bone BUA to be assessed (using the same echo signal). Specifically, the method is based on an algorithm that accounts for the distortion of the measurement data due to shielding effect exerted by cortical bone on the cancellous bone that is of immediate diagnostic interest. More explicitly (see also flow diagram of Fig. 2), the parameters of the cortical layer, such as its thickness and acoustic wave velocity are determined first using the pulse-echo ultrasound signal. Next, using these two parameters, the two-way transmission function of the cortical layer is calculated. Then, the trabecular bone model parameters, including BUA, are adjusted to obtain the best fit of the two spectra: the spectrum of the simulated scattered signal and the spectrum of the actually measured signal corrected for the impact of the cortical layer. Once the best fit procedure is completed it yields the BUA value of the cancellous bone, only. As mentioned earlier, such procedure, to the best of the authors' knowledge was not previously reported. As described in the following, the method was tested using pulse-echo measured data obtained at 1 MHz frequency for a custom designed bone mimicking phantom and a calf femur and provided consistent results.

In the next section, the underlying fundamentals of the procedure (also referred to as dual-spectrum approach [16]) including the model of ultrasound wave propagation and interaction with a multilayer structure are discussed along with the flow diagram depicting its step-by-step implementation. Next, experimental set-up enabling the pulse-echo measurements of investigated samples is described. In Section 4, experimental data evidencing the performance of the proposed method for artificial and animal bone samples are discussed. The conclusions of this study are summarized in Section 5.

2. Theory

Prior to discussion of the analysis that yielded the modified value of the cancellous bone attenuation and to gain an insight into the correction methodology developed it might be appropriate to consider the flow diagram shown in Fig. 2. This flow diagram depicts the step-by-step approach, in which the specific set of ultrasound generated data was processed to yield the BUA value accounting for the shielding contribution of the cortical bone.

To determine BUA for the purpose of this study from pulse-echo measurements the dual spectrum method presented in [16] was adapted. In [16] the method was used in the analysis of ultrasound echoes scattered by soft tissues (breast, liver) for tissue characterization. The modification involved comparison of echo data from examined bone specimen with the data recorded from a reference phantom whose attenuation coefficient was known. To this end, assuming $S_r(f, z)$ and $S_s(f, z)$, f being the frequency, correspond to the spectra of backscattered signals measured with the reference phantom and cancellous bone specimen at the penetration depth z, logarithm $S(f, z)$ of the spectral ratio was first computed:

$$S(f, z) = \log_e(S_s(f, z)/S_r(f, z)). \quad (1)$$

As discussed below, this logarithm is fitted to analytical model (defined later in this section).

As noted earlier, the spectrum $S_s(f, z)$ in Eq. (1) corresponds to the backscattered signal measured for the cancellous bone specimen. However, this is not the case in clinical applications due to the presence of the cortical bone, which influences the backscattered signal and its spectrum. To account for this influence in this study a method which allows compensation due to the cortical layer was developed. Specifically, to compensate for the cortical bone, the two-way propagation of the acoustic wave through the cortical layer was examined. For this purpose bone structure was approximated by a multilayered system (Fig. 2):

As further discussed in Section 3 this multilayered model was used because it resembles closely bone mimicking phantom construction; it is also adequate to represent calf femur sample (see Section 3.1). The probing ultrasound pulse wave was assumed to be propagating in water in the direction normal to the surface of the cortical bone; correspondingly, in the measurements conducted in-vitro using bone-mimicking phantom and calf bone sample 1 MHz ultrasound transducer was coupled to the bone through the water) (see discussion in Section 3.2). The model of Fig. 2 assumes that the cortical and cancellous bones can be represented by a homogeneous layers with clearly defined regular boundaries (parallel surfaces) and with specific mass densities

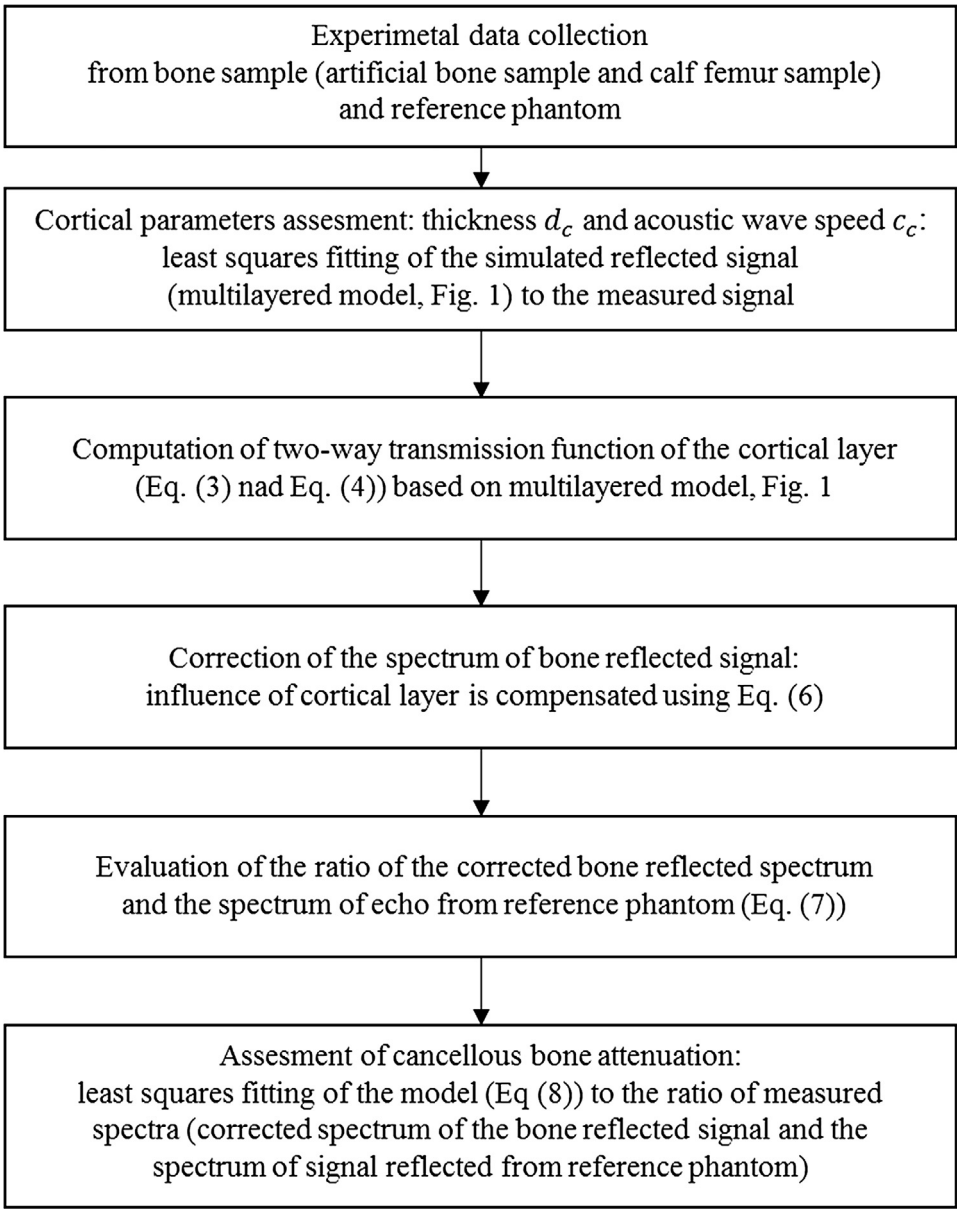

Fig. 1. Flow diagram showing the successive steps of the developed method of cancellous bone attenuation assessment with cortical bone influence correction.

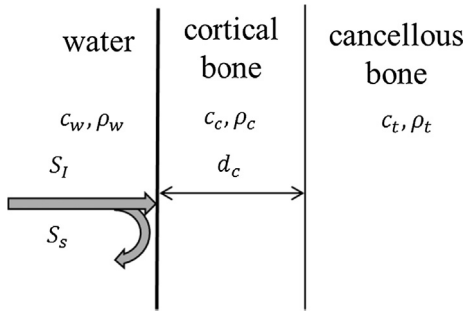

Fig. 2. Multilayered model of the real bone structure. Gray arrows indicate incident (S^I) and back-scattered (S_s) waves.

(cancellous: $\rho_t = 1020$ kg/m^3 for foam-like reference phantom and $\rho_t = 1150$ kg/m^3 for bone sample; cortical: $\rho_c = 1640$ kg/m^3 for bone phantom and $\rho_c = 1600$ kg/m^3 for bone sample, see Section 3.1) and frequency dependent acoustic wave velocities. Therefore, this model does not account for the effect of irregular boundaries such as those observed in cortical bone trabecularization. Moreover, to further simplify the analysis, only slow longitudinal wave (average value of wave velocity around 1550 m/s [17]) was considered to travel in the cancellous bone; the fast wave (average value of wave velocity around 2250 m/s [17]) amplitude was neglected (the ratio of the fast to slow amplitudes of longitudinal waves in trabecular bone ranges from -28 to -34 dB for porosities varying from 70 to 80%, as reported in [18]) amplitude was neglected. The implications of these simplifications are further discussed in the section Conclusions.

With the assumptions discussed above, the spectrum of the signal backscattered from the examined sample can be expressed as:

$$S_s(f) = R(f)S_I(f), \tag{2}$$

where $S_I(f)$ denotes the spectrum of the interrogating pulse wave and $R(f)$ is the reflection coefficient of the multilayered media (Fig. 2) (defined later in this Section). The two-way transmission function for the model shown in Fig. 2 was defined as:

$$T(f) = T_{wt}(f)T_{tw}(f) \tag{3}$$

where $T_{wt}(f)$ and $T_{tw}(f)$ are the frequency dependent transmission

functions of the cortical bone layer for the forward and backward propagating waves, respectively. For the model used here, analytical expressions for $T_{wt}(f)$ and $T_{tw}(f)$ were defined as [19]:

$$T_{tw}(f) = \frac{2Z_w}{S_{21}+S_{22}Z_w + (S_{11} + S_{12}Z_w)Z_t},\ T_{wt}(f) = \frac{2Z_t}{S_{21}+S_{22}Z_t + (S_{11} + S_{12}Z_t)Z_w}, \quad (4)$$

where $Z_w = \rho_w c_w$, $Z_t = \rho_t c_t$ denote the acoustic impedance of water and trabecular bone, respectively; ρ is the mass density; and c is the acoustic wave velocity. In Eq. (4), S_{ij} denotes the elements of the transmission matrix of the cortical layer given by:

$$S=\begin{bmatrix} S_{11} & S_{12} \\ S_{21} & S_{22} \end{bmatrix} = \begin{bmatrix} \cos k_c d_c & \frac{j}{Z_c}\sin k_c d_c \\ jZ_c \sin k_c d_c & \cos k_c d_c \end{bmatrix} \quad (5)$$

In the above equation, k_c and $Z_c = \rho_c c_c$ represent the wave number and acoustic impedance of the cortical bone, respectively and d_c is the thickness of the cortical layer. According to Eq. (5) the transmission functions of cortical bone layer, given by Eqs. (3) and (4), depend on the layer parameters, such as thickness and longitudinal wave velocity, which are usually unknown in real life measurements. The method developed here allows this issue to be alleviated. Specifically, the cortical bone thickness and longitudinal wave velocity were determined first using a method reported in [14]. This method is based on fitting the spectrum of the simulated reflected signal, obtained from a multilayered model shown in Fig. 2, to the spectrum of the measured bone reflected signal. The simulated reflected signal is obtained using Eq. (2) of [20], where the analytical solution for the reflection coefficient $R(f)$ is used (see Eq. (2) in [20]):

$$R(f) = \frac{S_{21}+S_{22}Z_t - (S_{11} + S_{12}Z_t)Z_w}{S_{21}+S_{22}Z_t + (S_{11} + S_{12}Z_t)Z_w},$$

The benefit of using this approach is that it allows the parameters of the cortical layer (required for backscattered signal spectrum correction) to be determined prior to the compensation of the cortical bone influence on the BUA assessment from single pulse-echo measurement. Specifically, once the cortical bone parameters are obtained, the two-way transmission function can be computed from Eqs. (3) and (4). To compensate for the influence of the cortical bone layer, the corrected spectrum of the measured backscattered signal defined as:

$$S_s^c(f, z) = \frac{S_s(f, z)}{T(f)}, \quad (6)$$

was substituted into Eq. (1) instead of $S_s(f, z)$ – the spectrum of measured backscattered signal. This substitution yielded the following expression:

$$S'(f, z) = \log_e(S_s^c(f, z)/S_r(f, z)), \quad (7)$$

The spectra ratio $S'(f, z)$ was then approximated by previously derived three parameters analytical model $\hat{S}(f, z)$ [16]:

$$\hat{S}(f, z) \equiv b + n\log_e f - 4\alpha f z. \quad (8)$$

Eq. (8) is a consequence of the frequency dependent backscatter coefficient $B(f) \approx bf^n$, which was confirmed experimentally in [21]. Moreover, as reported in [22], the attenuation coefficient in trabecular bone exhibits a linear relationship over the frequency range 0.2–1.7 MHz. Hence, linear frequency dependence is described by a factor of $e^{-4\alpha f z}$, where α is an effective attenuation coefficient. In Eq. (8), the parameters of the model are defined as follows:

$$b \equiv \log_e \frac{b_s}{b_r};\ n \equiv n_s - n_r;\ \alpha \equiv \alpha_s - \alpha_r. \quad (9)$$

In the above equation (Eq. (9)), the subscripts s, r correspond to the examined cancellous bone specimen and the reference phantom, respectively.

To determine the unknown coefficients (defined in Eq. (9)) of the model $\hat{S}(f, z)$, the least squares method was applied to fit it to the measured spectra ratio$S(f, z)$, denoted as:

$$\underset{b,n,\alpha}{\operatorname{argmin}} \sum_i (S'(f_i, z) - \hat{S}(f_i, z))^2. \quad (10)$$

The parameters of the cancellous bone b_s, n_s, $\alpha_s$were obtained by minimizing the least squared error in Eq. (10) making use of the simulated annealing algorithm (*simulannealbnd* routine from Matlab® Optimization Toolbox, MathWorks Inc., Natick, MA). Using corrected backscattered spectrum in Eqs. (7) and (10) allowed the influence of cortical bone on parameters b_s, n_s, α_s characterizing the cancellous bone to be compensated from a single pulse-echo measurement. Here, it is appropriate to note that in this study the attention was focused on determination of cancellous bone attenuation only, which was characterized by the model parameter α.

It is appropriate to note that the implementation of the algorithm presented in Fig. 1. is virtually instantaneous using Matlab (steps 2–5). Specifically, the processing time in Matlab® 8.5 on PC running Windows (Windows 10 × 64 with Athlon 64 X2 Dual Core 5600 + and core speed of 2.8 MHz) was about 3 sec.

3. Materials and methods

3.1. Samples

3.1.1. Reference phantom

As noted earlier, the proposed method requires the backscattered spectrum from the reference phantom to be known. Hence, well-documented sample of the porous material mimicking cancellous bone phantom was acquired from Sawbones (Sawbones, Pacific Research Laboratory Inc., Vashon, WA) was used (Fig. 3). Specifically, the cancellous bone-mimicking phantom was made of a cellular rigid polyurethane foam core whose structure resembles that of human cancellous bone.

To simplify comparison with the existing literature, the porosity of the cancellous bone mimicking foam sample (see next section) and the mass density of the foam core material were chosen to be $P = 90\%$ [23] (typical values of porosity for human bones range from 75% to 95% [24]) and $\rho_{core} = 1200$ kg/m^3 [23], respectively. The value of density of the cancellous bone mimicking material (used in multilayer model, see Section 2, Fig. 1), that is the foam saturated with water, was determined to be $\rho_t = 1020$ kg/m^3 :

$$\rho_t = (P\rho_w + (100 - P\rho_{core}))/100,$$

$\rho_w = 1000$ kg/m^3 being mass density of water. The value of acoustic wave velocity 1641 ± 4 m/s in the porous material (polyurethane foam) was obtained by measuring the difference in the time of arrival of an acoustic pulse travelling through the examined foam sample and travelling through distilled water of identical path length [25]. In the measurements the wave reflected from the ideal reflector placed on the bottom of the water tank was detected using a custom-made, 25 mm diameter focused transducer (see discussion in Section 3.2) with 50 mm focal distance and −3 dB focal zone of 58 mm. The transducer operated in pulse-echo mode and was excited by a sine cycle of 1 MHz frequency.

The frequency dependence of the attenuation coefficient of the reference phantom versus frequency, measured using a through-transmission method at a center frequency of 0.6 MHz, is shown in Fig. 3(b). The attenuation coefficient of the reference phantom obtained from the linear approximation was $\alpha_{ref} = 13$dB/MHz·cm (Fig. 3b). In this study, a similar slice of porous material was used as the reference phantom both for artificial bone and calf bone examination.

3.1.2. Artificial bone sample

As indicated in Fig. 2, the verification involved the use of the artificial and animal bone samples. The bone phantom materials used in

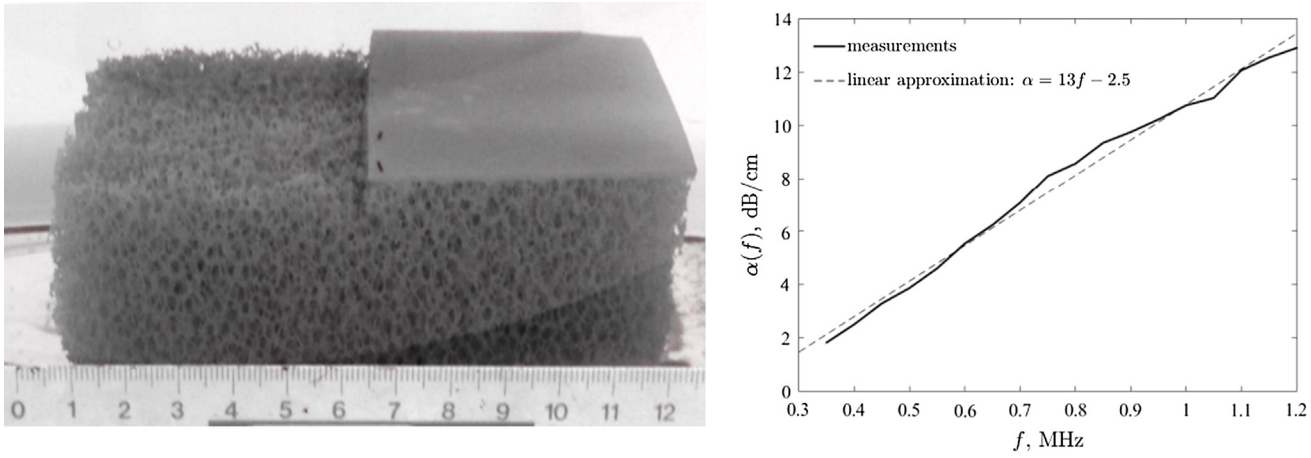

Fig. 3. (a) Reference phantom: Left hand side: top layer removed portion: porous (foam) material produced by Sawbones (Sawbones, Pacific Research Laboratory Inc., Vashon, WA). Right hand side portion shows artificial bone sample of 1 mm thickness plate made of oriented glass fibers mixed with epoxy (same vendor) and bonded to the same substrate of porous material. (b) Attenuation versus frequency for the reference phantom material. Dashed line shows the linear approximation used for comparison with attenuation of the artificial bone sample (see Section 4.2, Fig. 7(b)).

Table 1
Model parameters required for transmission function evaluation from Eq. (5) and Eq. (6) for the calf bone sample and corresponding midpoint and range values from the literature.

Parameter	Midpoint value (Range)
Cancellous characteristic impedance, kg/m^2 s $\times$ 10^6	1.87 (1.54–2.25)
Cancellous longitudinal wave velocity, c_t, m/s	1625 (1450–1800)
Cortical bone mass density ρ_c, kg/m^3	1600 (1330–2000)

the measurements reported here closely mimicked both the geometry and material properties of the cancellous and cortical bones. Specifically, the artificial bone was composed of a thin (1 mm) plate bonded to a substrate of porous (foam-like)) material, both produced by Sawbones (Sawbones, Pacific Research Laboratory Inc., Vashon, WA; Fig. 3a). More specifically, the cortical bone-mimicking 1 mm plate consisted of composite of glass fibers and epoxy resin, (again, both produced by Sawbones (Sawbones, Pacific Research Laboratory Inc., Vashon, WA). The material was transversely isotropic, with elastic properties close to those of real cortical bone; its mass density was 1640 kg/m^3 [23]. The cancellous bone-mimicking foam was made of a rigid polyurethane foam core. The same sample of the porous material was used as the reference phantom (Fig. 3a). The thickness of the porous material that modeled the cancellous bone was about 30 mm. This thickness allowed the backscattered signal from the region of interest (ROI) located at the depth of 10 mm to be obtained and the influence of the signal reflected from the rear surface of the foam to be minimized (due to attenuation at the two-way propagation distance of 60 mm). The acoustic parameters of the phantom materials were relevant to typical values observed in clinical practice (e.g., femoral neck [26]).

3.1.3. Calf femur bone sample

The correction method was also verified using experimental data obtained from a fresh (no longer than 6 h after slaughter) calf femur bone sample acquired from a local butcher. A proximal epiphysis part of the bone was separated and the scraps of soft tissue (like meat and fat) were carefully removed with scalpel so as not to damage the bone surface. Measurements were taken immediately after sample preparation so that the bone would not need to be frozen.

3.1.4. Material parameters of the model

The multilayered model shown in Fig. 2 was used to evaluate the two-way transmission functions using Eqs. (5) and (6). The following material parameters of the model were applied: water: mass density $\rho_w = 1000$kg/m^3 and acoustic wave speed $c_w = 1490$m/s (at the temperature of 23 °C used in experiments, see Section 3.2). For the artificial bone, the mass density of the cortical shell was assumed to be $\rho_c = 1640$kg/m^3 [23]. The averaged ($N = 24$; see Section 3.2) values of the cortical layer thickness and acoustic wave speed assessed using the method of [20] were $d_c = 1.08$ mm and $c_c = 3016$ m/s, respectively with the corresponding standard deviations of $\sigma_d = 0.06$mm and$\sigma_c = 52$m/s. The mass density of the cancellous bone mimicking foam was assumed to be $\rho_t = 1020$ kg/m^3 [23] and wave speed $c_t = 1641$m/s i.e. identical as for the reference phantom values (see Section 3.1.1).

For the calf bone sample, midpoint (defined here as $(V_{max} + V_{min})/2$, V_{max} and V_{min} being the limits of given range of corresponding values in Table 1) values were chosen from the ranges given in the literature [27]. These values were needed to calculate the two-way transmission functions of the cortical layer (Table 1) [27].

The cancellous bone mass density, which corresponded to the assumed values of the acoustic wave speed and characteristic impedance, shown in Table 1, was $\rho_t = 1150$ kg/m^3. The values of acoustic wave speed and cortical bone thickness were assessed using the method of simultaneous estimation of cortical bone parameters [20]. The corresponding averaged values ($N = 5$; see Section 3.2) and standard deviations were$d_c = 1.33$ mm, $\sigma_d = 0.09$ mm and $c_c = 2998$ m/s, $\sigma_c = 87$ m/s.

3.2. Experimental set-up and data processing

As noted earlier the methodology developed to mitigate the influence of cortical bone required the backscattered signals from both the examined bone specimen and reference phantom to be determined under identical conditions. That was done in experimental set-up shown in Fig. 4. The reference phantom and examined samples were immersed in distilled water at room temperature (23 °C). The measurements were made with the ultrasound transmit–receive system shown in Fig. 4, which allowed the instrumentation-dependent factors that influence the backscattered spectra from both the reference and examined specimens to be cancelled [16]. The measurements were taken with the same 1 MHz custom-made transducer. The focused transducer was used to achieve focusing of the transmitted signal energy in the ROI in cancellous bone (shielded by the cortical layer). This focusing assured that the influence of the reflected signals originating from the regions located outside the ROI was minimized due to minimization of transmit

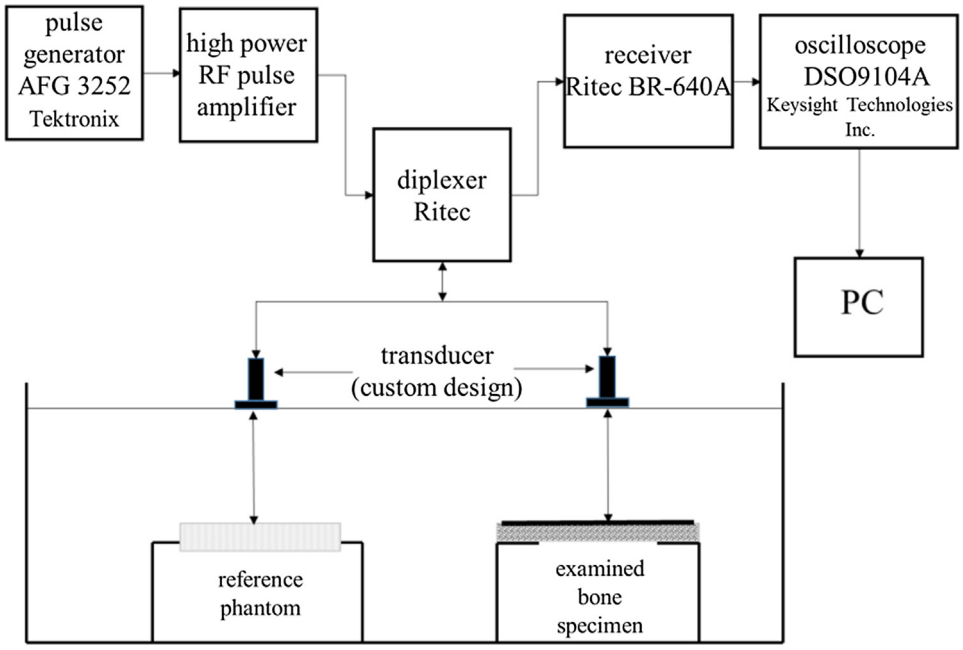

Fig. 4. Schematic diagram of experimental ultrasound measurement set-up.

wave-beam diffraction in the transducer focus. At the same time, the signal reflected from the ROI was maximized due to focusing. The transducer operated in pulse-echo mode and was excited by a sine cycle of 1 MHz frequency. Experimental setup and the probing wave parameters were typical of those used for BUA measurements (in transmission mode) (typical frequency range from 0.2 MHz to 1.5 MHz [28]) where the patient's part of the body (hip, spine, humerus etc.) being examined is coupled though water bath or ultrasound gel. The transmitted pulse was obtained using a pulse generator (Tektronix AFG 3252 dual-channel arbitrary function generator, Tektronix GmbH, Germany, Köln) and then a custom-designed high-power RF pulse amplifier. The 15 MHz bandwidth custom designed High Power RF amplifier was capable of delivering 10 W linear power output and allowed required transmit pulse parameters to be obtained while minimizing undesirable heating effects and parasitic excitations at harmonic frequencies.

The reflected signals were detected using the same ultrasound transducers switched to the receive mode (Ritec RDX-2 diplexer, SINCOS Analytics LLC Berlin, Germany). The waveform of interrogating pulse was determined using the echo reflected from 30 mm thick brass plate positioned at the axial distance of 50 mm corresponding to the focal distance of the 1 MHz transducer (water-brass acoustic wave reflection coefficient at normal incidence is 0.92). The spectra needed to be inserted in Eq. (10) were calculated from the time-gated signals backscattered from the reference phantom and the examined bone specimen. This is illustrated in Fig. 5, where the corresponding waveforms for the reference foam and artificial bone sample are shown. The two time windows shown in Fig. 5(a) and (b) had the same duration $\Delta\tau = 10\mu$s and the same time delay $\tau = 10\mu$smeasured from the front surface of the samples. The parameters $\Delta\tau$ and τ were related to the center of the region of interest (ROI) located at the depth $z = 12$ mm (see discussion below) and the transducer center frequency $f_0 = 1$MHz.

The time window $\Delta\tau$ equal to ten cycles of the transducer center frequency $f_0 = 1$MHz was selected for analysis, yielding$\Delta\tau = 10\mu$s. This selection was based on the results of Hoffmeister et al. [29] who determined the time window by trial and error method. To eliminate dependence of the spectrum of time-windowed signal on $\Delta\tau$ it was normalized by the value of $\Delta\tau$ [29]. The position of the ultrasound probe was adjusted manually to obtain focusing at the depth $z \approx 12$mm measured from the bone surface, which corresponded to the center of the ROI in the cancellous site at the depth of10mm (assuming the cortical thickness to be approximately 2mm). This choice of ROI ($z = 12$ mm) and corresponding delay τ ensured that no energy from the surface reflection from the cortical bone was included in the time window $\Delta\tau$, selected for BUA assessment. For the specified ROI location, the corresponding time delay $\tau = 10\mu$s was obtained.

To minimize spatial variability of the backscattered signal from porous material (foam) modeling the cancellous bone, the measurements of the backscattered signals for the reference foam and artificial bone specimen were taken at 24 distinct points spaced at 5 mm along direction perpendicular to the plane plane being imaged (see Fig. 4) and passing through the centers of the samples (reference foam and bone phantom). This allowed the whole sample to be covered. The 5 mm separation corresponded to approximate value of the -3 dB focal lateral beam-width of the 1 MHz source used in the measurements, which assured acoustic beams separation for individual measurements at distinct measurement points. The spectra were then corrected using Eq. (6) and the average spectrum for the artificial bone sample was evaluated. Next, the cancellous bone attenuation, which was characterized by the model parameter, $\alpha$was obtained from Eq. (8) for both the corrected and non-corrected spectra.

Similarly, in the case of the calf bone specimen, to cover the whole flat area on the surface of the bone specimen the measurements of the backscattered signal were taken at five points spaced every 5 mm. Again, the spectra were corrected and averaged. Subsequently, the cortical layer of bone sample was removed carefully and the measurements of the backscattered signal from the cancellous bone alone were repeated at the same reference position of the transducer. The spectra from the total bone sample and cancellous bone alone have been used to determine the attenuation coefficient.

In Fig. 6a, examples of the averaged spectra of the signal backscattered from the artificial bone sample $S_s(f)$ and from the reference foam $S_r(f)$ are shown. The thin solid line shows the averaged spectral ratio, which was fitted to the model defined in Eq. (3). Data fitting was performed in the limited frequency range, which corresponded to -3 dB bandwidth of the transmitted pulse (thin solid line; Fig. 6b), ranging from 0.85 MHz to 1.15 MHz. Examples of the transfer function $1/T(f)$, required to obtain the corrected spectrum from Eq. (5), are shown for various thicknesses of the cortical layer $d_c = (1.08, 1.5$and2mm) at an acoustic wave speed of $c_c = 3016$ m/s, which corresponds to the assessed value of the wave speed in cortical

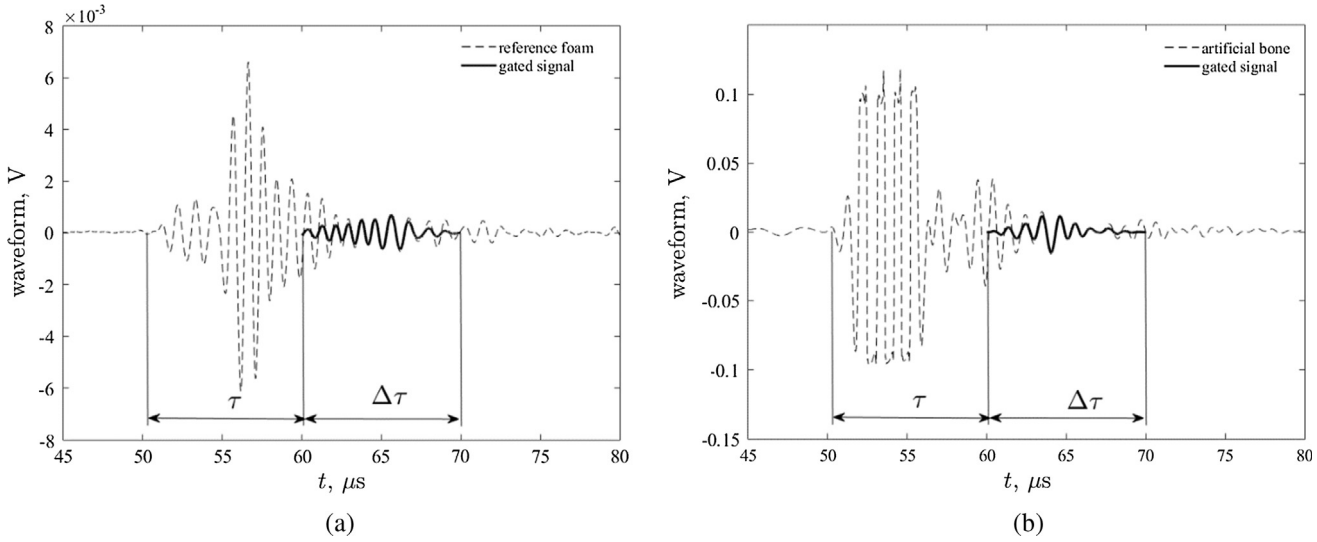

Fig. 5. Backscattered waveforms from the (a) reference phantom and (b) artificial bone sample. Solid line indicates the gated part of the signal from the chosen (here 12 mm) depth, which is utilized in the dual-spectrum method to assess the attenuation of the cancellous bone.

bone mimicking plate (see Section 3.1.4). In this frequency band, the shape of the transmission function depends on cortical layer thickness (d_c).

4. Results and discussion

4.1. Artificial bone

In Fig. 7a, examples of the measured backscattered signals spectral ratio $S(f, z)$ and its approximation by the model defined in Eq. (2) are shown for the artificial bone sample. The frequency-dependent attenuation coefficient is shown in Fig. 7b)

In Fig. 7b the solid black line corresponds to the attenuation coefficient obtained after applying the correction procedure and the dashed grey line represents the attenuation coefficient of the reference phantom (see Fig. 3b). The attenuation coefficients determined were α_{sample} = 13.5dB/MHz·cm and α_{ref} = 13dB/MHz·cm, with a relative error of 3.9%. For comparison, the attenuation coefficient obtained without correction is also presented (dashed black line). The non-corrected attenuation coefficient was found to be α_{sample} = 14.07dB/MHz·cm, with the corresponding error of 8.3%. The root-mean-square deviation (RMSD) between the estimated attenuation coefficient obtained for the corrected spectrum and the coefficient obtained for the reference phantom was calculated to be equal to RMSD = 0.51 dB/cm. The corresponding value obtained for the non-corrected spectrum was RMSD = 0.97 dB/cm.

4.2. Calf bone

The method was also tested using the measured backscattered signals obtained for the calf bone sample. Specifically, the spectral ratio $S(f, z)$ and its approximation by the model, Eq. (2), are shown (Fig. 8a). In Fig. 8b, the frequency-dependent attenuation coefficient is shown.

The grey line represents the value of attenuation for the calf bone specimen after the cortical layer has been removed ($\alpha_{cancellous}$; Fig. 8b) and the solid black line represents the attenuation coefficient obtained for the bone sample using corrected backscattered spectrum. The attenuation coefficients were calculated to be α_{sample} = 21.7 dB/MHz·cm and $\alpha_{cancellous}$ = 20.7dB/MHz·cm, with a relative error of 4.7%. For comparison, the dashed black line represents the attenuation coefficient

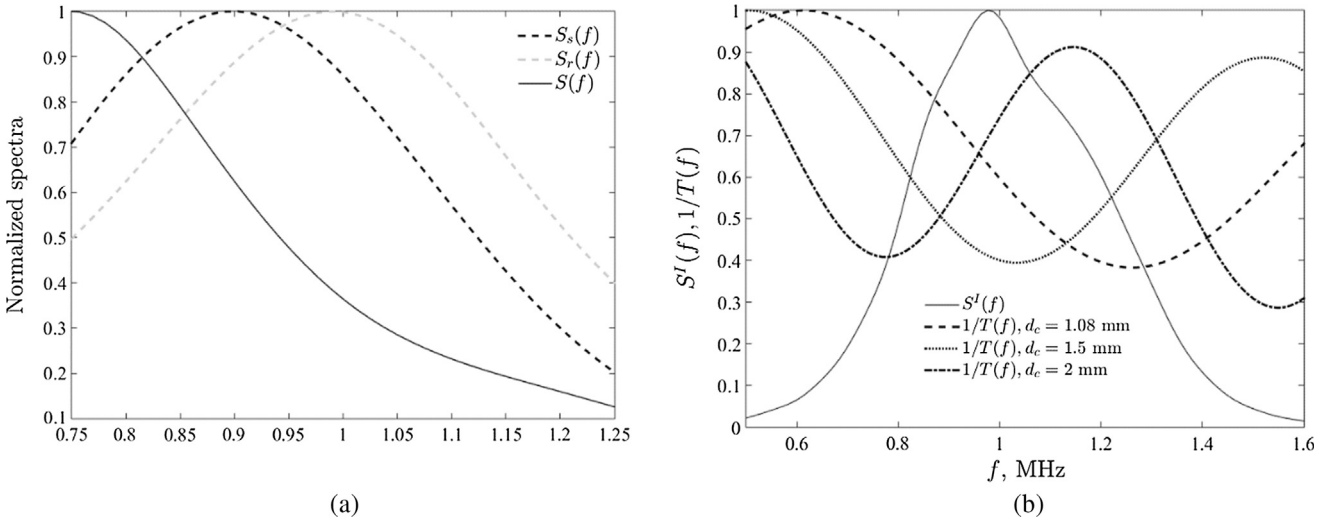

Fig. 6. (a) Example of the spectra averaged from 24 measurements of the signals backscattered from the examined artificial bone $S_s(f)$ and from the reference phantom $S_r(f)$; $S(f) = \log_e(S_s(f, z)/S_r(f, z))$. (b) The normalized magnitude of the two-way transmission function $1/T(f)$ (Eq. (5)) for different thickness values, d_c; the acoustic wave speed in the cortical bone c_c = 3016 m/s; $S^I(f)$ – incident wave spectrum.

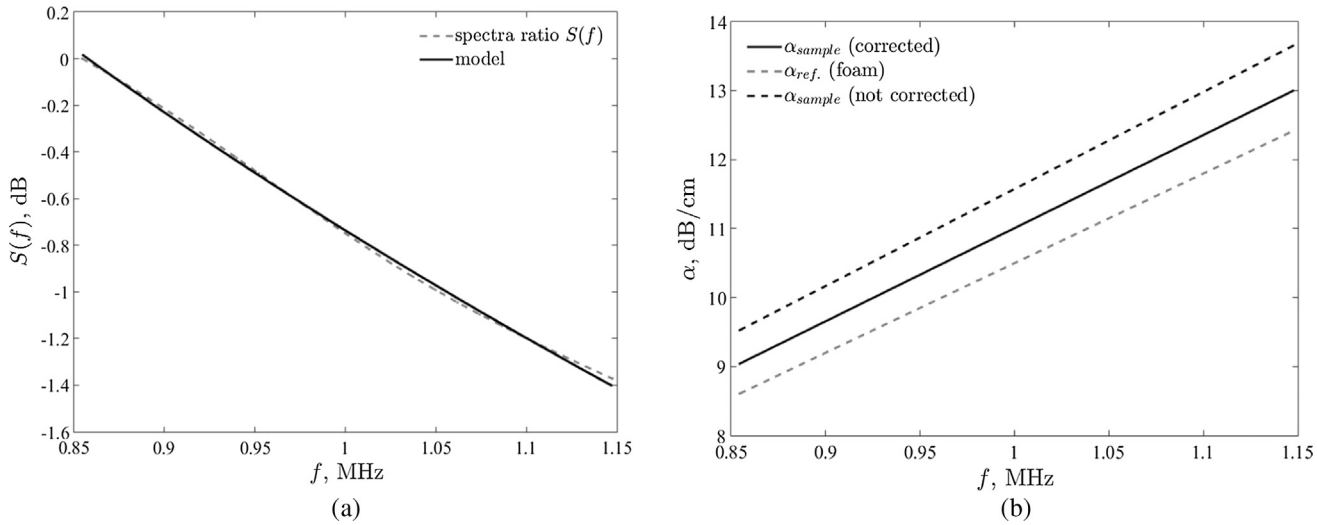

Fig. 7. (a) Measured and fitted spectral ratio $S(f, z)$ and (b) attenuation coefficient as the function of frequency for the artificial bone.

obtained when the spectra ratio was computed using the non-corrected backscattered spectrum. In this case, the attenuation coefficient was α_{sample} = 22.6dB/MHz·cm, and the error was 9.2%. The RMSD between the estimated attenuation coefficient obtained for corrected spectrum and the true value obtained for the cancellous bone with cortical layer removed was RMSD = 0.97 dB/cm. The corresponding value for the non-corrected spectrum (dashed black line; Fig. 8b) was RMSD = 1.89 dB/cm.

5. Conclusions

The results presented confirmed that the procedure developed allowed the corrected value and parameter of the cancellous bone (BUA) to be determined simultaneously from the single (pulse-echo) bone backscattered wave. The validity of the method was tested using acoustic data obtained from a custom-designed bone-mimicking phantom and a calf femur. The relative error of the attenuation coefficient assessment was determined to be 3.9% and 4.7% for the bone phantom and calf bone specimens, respectively. When the cortical shell influence was not taken into account the corresponding errors were considerably higher: 8.3% (artificial bone) and 9.2% (calf femur).

As indicated earlier one of the motivations of this work was to examine whether ultrasonically evaluated or monitored osteoporosis could be developed to be clinically accepted providing non-ionizing alternative to DEXA methodology. Such alternative would also be desirable because in contrast to DEXA, ultrasound equipment is inexpensive and fully portable. Moreover, in many cases like in cancellous bone evaluation of neonates or in bone status screening, the QUS techniques can be considered as inexpensive non-ionizing alternative of DEXA. If clinically proven, the use of the BUA measurement technique in reflection mode would augment diagnostic power of the attending physician by permitting to include bones, which are not accessible for through transmission mode, e.g. hip, spine, humerus and femoral neck. However, the presently available ultrasound methods are not capable to determine directly the values of bone mineral density (BMD) or bone mineral content (BMC) needed to diagnose the level (or stage) of osteoporosis. In currently acceptable clinical practice, such diagnosis is rendered based on the outcome of DEXA scan using T-score value as indicative of the risk of developing a fracture. The T-score is related to a number of standard deviations below T = −1. The value of T = −1 corresponds to normal mean results obtained through examination of young healthy adults. Whereas the score higher than −1 is considered to be normal, a score ranging between −1 and −2.5 indicates osteopenia (low bone mass). A T-score below −2.5 is defined as osteoporosis. The in-vitro results presented in Section 3 show relatively good correlation between quantitative ultrasound (QUS) indices and bone

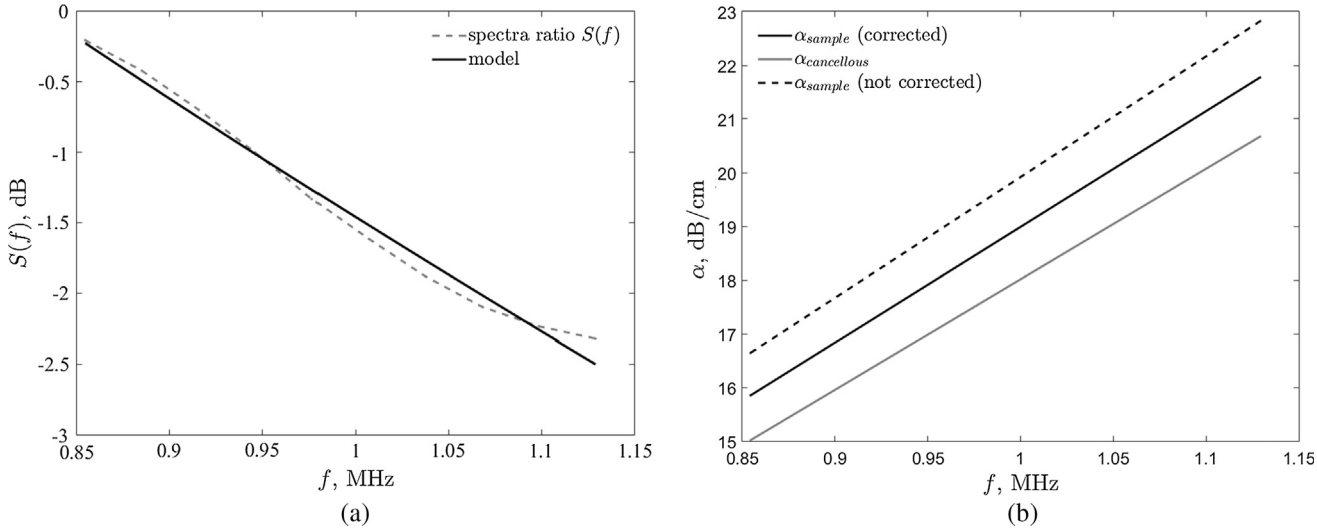

Fig. 8. (a) Measured and fitted spectral ratio $S(f, z)$ and (b) attenuation coefficient as the function of frequency for the calf bone specimen.

mineral density (BMD) (R = 0.86 for Speed of Sound, SoS and R = 0.8 for broadband ultrasound attenuation, (BUA) [6], however, the corresponding correlation coefficients for in-vivo data are considerably lower: correlation coefficient between femoral BMD and BUA and SoS were determined to be R = 0.4–0.61 and R = 0.3–0.55, respectively [30]). Such large difference indicates that the existing ultrasound methods are not immediately likely to replace the DEXA technique. This preliminary conclusion is further supported by the fact that *in-vivo* results reported in the literature also show relatively low correlation between QUS parameters measured using pulse-echo method and BMD Specifically, the correlation coefficient between average backscatter coefficient (ABC) and calcanea BMD was determined to be R = 0.5 [31], correlation between apparent integrated backscatter (AIB) and femoral BMD was determined to be R = 0.52 [32] and the correlation coefficient between broadband ultrasound backscatter (BUB) and BMD varied from 0.34 for femur BMD [11] to 0.87 [33] for calcaneus BMD. The relatively high correlation (0.87) reported in [33] was determined using data acquired from 10 healthy human volunteers and therefore the results might not be relevant for osteoporotic fracture risk prediction. The correlation between other pulse-echo measured parameters like, frequency slope of apparent backscatter (FSAB), time slope of apparent backscatter (TSAB) or broadband ultrasound attenuation (BUA), reported in this work, and bone mineral density (BMD) or bone mineral content (BMC) have not yet been established. Hence, the summarized above discrepancies, together with the technical difficulties of pulse-echo (PE) measurements *in-vivo*, suggest that the PE ultrasound determined QUS parameters currently available, are not adequately consistent to be clinically acceptable for prediction of the BMD or BMC. There is also lack of “T-like” universal index; development of such ultrasound osteoporosis index would involve the need of its verification in a substantial number of patients.

It should also be pointed out that although the outcome of this work verified that the shielding effect of cortical bone on assessed value of BUA in the cancellous bone can be accounted for, the model used in this work was not completely adequate to mimic the examined bone mechanical structure (and hence its mechanical strength) due to the simplifications pointed out in Section 2. Therefore, at this juncture, the method described may only be considered as an incremental contribution to the development of clinically acceptable alternative to DEXA.

As discussed earlier, in general, the correlation coefficients determined using pulse-echo method are not sufficiently high to be deemed clinically applicable. Thus, it is unlikely that a single ultrasonically obtained parameter can be considered as adequate to be equivalent to DEXA’s method T-score. However, it is conceivable that the T-score might be replaced with the QUS determined “composite” or “effective” index. Such index is yet to be developed and then verified in-vivo, so the correlation between the assessed BUA and BMD can be established.

References

[1] H.K. Genant, S. Grampp, C.C. Glüer, K.G. Faulkner, M. Jergas, K. Engelke, C. Van Kuijk, Universal standardization for dual X-ray absorptiometry: patient and phantom cross-calibration results, J. Bone Miner. Res. 9 (10) (1994) 1503–1514.

[2] H.K. Genant, J.E. Block, P. Steiger, C.C. Glueer, R. Smith, Quantitative computed tomography in assessment of osteoporosis, Semin. Nucl. Med. 17 (4) (1987) 316–333.

[3] A.J. Yates, P.D. Ross, E. Lydick, R.S. Epstein, Radiographic absorptiometry in the diagnosis of osteoporosis, Am J. Med. 98 (2A) (1995) 41S–47S.

[4] M. Boyanov, Forearm single X-ray absorptiometry in the identification of postmenopausal women with osteoporosis at the hip and spine: a correlation study, J. Clin. Densitom. 8 (4) (2005) 423–429.

[5] F. Padilla, F. Jenson, V. Bousson, F. Peyrin, P. Laugier, Relationships of trabecular bone structure with quantitative ultrasound parameters: in vitro study on human proximal femur using transmission and backscatter measurements, Bone 42 (6) (2008) 1193–1202.

[6] K.A. Wear, S. Nagaraja, M.L. Dreher, S.L. Gibson, Relationships of quantitative ultrasound parameters with cancellous bone microstructure in human calcaneus in vitro, J. Acoust. Soc. Am. 131 (2) (2012) 1605–1612.

[7] D. Hans, P. Dargent-Moline, A. Schott, J. Sebert, C. Cormier, P. Kotski, et al., Ultrasonographic heel measurements to predict hip fracture in elderly women: the Epidos prospective study, Lancet 348 (9026) (1996) 511–514.

[8] P. Thomson, J. Taylor, R. Oliver, A. Fisher, Quantitative ultrasound (QUS) of the heel predicts wrist and osteoporosis related fractures in women ages 45–75 years, J. Clin. Densitometry 1 (1998) 219–225.

[9] E.M. Lewiecki, N.C. Wright, J.R. Curtis, E. Siris, R.F. Gagel, K.G. Saag, A.J. Singer, P.M. Steven, R.A. Adler, Hip fracture trends in the United States, 2002 to 2015, Osteoporosis Int. 29 (2018) 717–722.

[10] J.A. Kanis, Osteoporosis, Blackwell Science, 1994, p. 85.

[11] C. Roux, V. Roberjot, R. Porcher, S. Kolta, M. Dougados, P. Laugier, Ultrasonic backscatter and transmission parameters at the os calcis in postmenopausal osteoporosis, J. Bone Miner. Res. 16 (7) (2001) 1353–1362.

[12] T. Tang, Ch. Liu, F. Xu, D. Ta, Correlation between the combination of apparent integrated backscatter–spectral centroid shift and bone mineral density, J. Med. Ultrasonics 43 (2016) 167–173.

[13] B.K. Hoffmeister, D.P. Johnson, J.A. Janeski, D.A. Keedy, B.W. Steinert, A.M. Viano, S.C. Kaste, Ultrasonic characterization of human cancellous bone in vitro using three different apparent backscatter parameters in the frequency range 0.6–15MHz, IEEE Trans. Ultrason. Ferroelectr. Freq. Control. 55 (7) (2008) 1442–1452.

[14] Y. Xia, W. Lin, Y.X. Qin, The influence of cortical end-plate on broadband ultrasound attenuation measurements at the human calcaneus using scanning confocal ultrasound, J. Acoust. Soc. Am. 118 (3 Pt 1) (2005) 1801–1807.

[15] J. Litniewski, A. Nowicki, A. Sawicki, Detection of bone disease with ultrasound-comparison with bone densitometry, Ultrasonics 38 (2000) 693–697.

[16] K. Nam, J.A. Zagzebski, T.J. Hall, Simultaneous backscatter and attenuation estimation using a least squares method with constraints, Ultrasound Med. Biol. 37 (12) (2011) 2096–2104.

[17] J.J. Hoffman, A.M. Nelson, M.R. Holland, J.G. Miller, Cancellous bone fast and slow waves obtained with Bayesian probability theory correlate with porosity from computed tomography, J. Acoust. Soc. Am. 132 (3) (2012) 1830–1837.

[18] Y. Nagatani, K. Mizuno, T. Saeki, M. Matsukawa, T. Sakaguchi, H. Hosoi, Propagation of fats and slow waves in cancellous bone: comparative study of simulation and experiment, Acoust. Sci. Technol. 30 (4) (2009) 257–264.

[19] P.R. Stepanishen, Reflection and transmission of acoustic wideband plane waves by layered viscoelastic media, J. Acoust. Soc. Am. 71 (1) (1982) 9–21.

[20] Y. Tasinkevych, J. Podhajecki, K. Falińska, J. Litniewski, Simultaneous estimation of cortical bone thickness and acoustic wave velocity using a multivariable optimization approach: bone phantom and *in vitro* study, Ultrasonics 65 (2016) 105–112.

[21] K.A. Wear, Frequency dependence of ultrasonic backscatter from human trabecular bone: theory and experiment, J. Acoust. Soc. Am. 106 (6) (1999) 3659–3664.

[22] S. Chaffai, F. Padilla, G. Berger, P. Laugier, In, vitro measurement of the frequency-dependent attenuation in cancellous bone between 0.2 and 2 MHz, J. Acoust. Soc. Am. 108 (3) (2000) 1281–1289.

[23] https://www.sawbones.com/biomechanical/material-selection/.

[24] S. Chaffai, F. Peyrin, S. Nuzzo, R. Porcher, G. Berger, P. Laugier, Ultrasonic characterization of human cancellous bone using transmission and backscatter measurements: relationships to density and microstructure, Bone 30 (1) (2002) 229–237.

[25] G. Kossoff, E.K. Fry, J. Jellins, Average velocity of ultrasound in the human female breast, J. Acoust. Soc. Am. 53 (6) (1973) 1730–1736.

[26] K.E. Poole, P.M. Mayhew, C.M. Rose, et al., Changing structure of the femoral neck across the adult female lifespan, J. Bone Miner. Res. 25 (3) (2010) 482–491.

[27] P. Laugier, G. Haiat, Introduction to the physics of ultrasound, in: P. Laugier, G. Haiat (Eds.), Bone Quantitative Ultrasound, Springer, Netherlands, p. 39, 2011.

[28] K.-Y. Chin, S. Ima-Nirwana, Calcaneal quantitative ultrasound as a determinant of bone health status: what properties of bone does it reflect? Int. J. Med. Sci. 10 (12) (2013) 1778–1783.

[29] B.K. Hoffmeister, A.R. Wilson, M.J. Gilbert, M.E. Sellers, A backscatter difference technique for ultrasonic bone assessment, J. Acoust. Soc. Am. 132 (6) (2012) 4069–4076.

[30] C.F. Njeh, D. Hans, J. Li, B. Fan, T. Fuerst, Y.Q. He, E. Tsuda-Futami, Y. Lu, C.Y. Wu, H.K. Genant, Comparison of six calcaneal quantitative ultrasound devices: precision and hip fracture discrimination, Osteoporos. Int. 11 (2000) 1051–1062.

[31] K. Wear, D.W. Armstrong, Relationships among calcaneal backscatter, attenuation, sound speed, hip bone mineral density, and age in normal adult women, J. Acoust. Soc. Am. 110 (1) (2001) 573–578.

[32] J.P. Karjalainen, O. Riekkinen, J. Töyräs, M. Hakulinen, H. Kröger, T. Rikkonen, K. Salovaara, J.S. Jurvelin, Multi-site bone ultrasound measurements in elderly women with and without previous hip fractures, Osteoporos. Int. 23 (2012) 1287–1295.

[33] K. Wear, B. Garra, Assessment of bone density using ultrasonic backscatter, Ultrasound Med. Biol. 24 (5) (1998) 689–695.